

Second-order Statistics for Threat Assessment with the PHD Filter

Alexey Narykov^{1,2}, Emmanuel D. Delande¹, Daniel E. Clark¹, Paul Thomas³, and Yvan Petillot¹

¹Institute of Sensors, Signals and Systems, Heriot-Watt University, Edinburgh EH14 4AS, UK

²Institute for Digital Communications, University of Edinburgh, Edinburgh EH9 3FG, UK

³Cyber and Information Systems Division, Dstl Porton Down, Wiltshire SP4 0JQ, UK

Abstract—This paper explores application of the Probability Hypothesis Density (PHD) filter to the estimation of a threat level pertaining to an object population. Specifically, it develops explicit and compact expression for computation of its variance, a second-order statistical moment that quantifies the dispersion of the threat level around its mean value. The behaviour of the statistic is demonstrated through simulation examples.

I. INTRODUCTION

Successful operation of many civil and military command and control (C2) systems is defined by operator's ability to act in response to the results of automatic threat assessment based on sensor observations. In practice, assessment corresponds to computation of threat levels of objects in the surveillance area with respect to (w.r.t.) negative effects of their estimated or predicted behaviour [1], [2]. However, the operator's ability to act can be compromised in the following situations:

- when the number of objects in the surveillance area is too high, exceeding human cognitive capacities or leading to interferences in presentation of results [3];
- when threat level estimates are not equipped with a measure of their quality, rendering results unreliable or arguably meaningless [4, p. 150].

One way to address the first point above is to aggregate *individual* object threats [5], [6], [7] into a scalar-valued *population* threat that depends on the number and states of individual targets — ideally preserving the collective effects of underlying behaviours and interactions [8]. Building from his early works on multi-object detection/tracking for population of objects [9], Mahler proposed the expression of the first-order statistic of the population threat for multi-object filtering solutions derived from the Finite Set Statistics (FISST) framework, including the Probability Hypothesis Density (PHD) filter [9].

In order to address the second point above, this paper introduces the second-order statistic for a population threat, and illustrates this concept in the context of the PHD filter. This result builds upon the work of Delande et al. [10] on regional statistics that provide first- and second-order information on

the number of objects in an arbitrary region of the surveillance area.

Section II covers the necessary background material on multi-object Bayesian estimation with point processes, and describes the PHD filter. Section III defines the aggregate threat function and its statistics, and exploits them to extract threat statistics from the output of the PHD filter. Numerical examples are given in Section IV. Section V concludes the paper. The proofs of the results in Section III are given in the Appendix.

II. MULTI-OBJECT BAYESIAN FILTERING

This section presents background and notation used throughout the article. Point processes are briefly described in Section II-A and Section II-B provides a description of the PHD filter.

A. Point Processes

In this article, the objects of interest have individual states x in some d -dimensional state space $\mathbf{X} \subset \mathbb{R}^d$, typically consisting of position and velocity variables. A point process Φ on \mathbf{X} is a random variable on the process space $\mathcal{X} = \bigcup_{n=0}^{\infty} \mathbf{X}^n$, i.e. the space of all finite sequences of points in \mathbf{X} , whose number of elements *and* element states are unknown and (possibly) time-varying. A realisation of Φ is a sequence¹ $\varphi = (x_{1:n}) \in \mathbf{X}^n$, representing a population of n objects with states $x_i \in \mathbf{X}$. In the context of multi-object filtering, this sequence depicts a specific multi-object configuration.

More formally, a point process Φ on \mathcal{X} is a measurable mapping

$$\Phi : (\Omega, \mathcal{F}, \mathbb{P}) \rightarrow (\mathcal{X}, \mathcal{B}(\mathcal{X})) \quad (1)$$

from some probability space $(\Omega, \mathcal{F}, \mathbb{P})$ to the measurable space $(\mathcal{X}, \mathcal{B}(\mathcal{X}))$, where Ω is a sample space; \mathcal{F} is a σ -algebra on Ω ; \mathbb{P} is a probability measure on (Ω, \mathcal{F}) ; $\mathcal{B}(\mathcal{X})$ is the Borel σ -algebra on \mathcal{X} [11].

As for usual real-valued random variables, a point process is described by its probability distribution P_Φ on \mathcal{X} . The probability distribution is always defined as a symmetric function, so that the order of points in a realisation is irrelevant for statistical purposes and the permutations of φ —such as (x_1, x_2) and (x_2, x_1) —are equally probable. In addition, a

This work was supported by the Engineering and Physical Sciences Research Council (EPSRC) Grant number EP/K014277/1 and the MOD University Defence Research Collaboration (UDRC) in Signal Processing.

Corresponding author: Alexey Narykov, email: an23@hw.ac.uk.

¹In this paper $(x_{1:n})$ denotes the sequence (x_1, \dots, x_n) .

point process is called *simple* if the probability distribution is such that realisations are sequences of points that are pairwise distinct almost surely, i.e. φ does not contain repetitions. For the rest of the paper, all the point processes are assumed simple².

Throughout the paper all random variables are defined on $(\Omega, \mathcal{F}, \mathbb{P})$. $\mathbb{E}[\cdot]$ and $\text{var}[\cdot]$ denote, respectively, the expectation and the variance w.r.t. \mathbb{P} . In order to describe real-valued random variables on \mathbb{R}_0^+ and random variables on \mathbf{X} , these spaces are equipped with their corresponding Borel σ -algebras.

B. The Probability Hypothesis Density Filter

In the context of Bayesian multi-object filtering, Φ_k describes the information about the object population known by the operator at time k . Multi-object Bayes' filter, in its most general form, cannot be implemented in a computationally tractable manner even for a small number of objects [13]. Its most popular approximation is perhaps the PHD filter [12]. The PHD filter propagates the density of the first-order factorial moment of the point process Φ_k , denoted by μ_k , and also called the Probability Hypothesis Density (PHD) or intensity function. The PHD filter recursion at time step k consists of a time prediction step and a data update steps given by [12]

$$\mu_{k|k-1}(x) = \mu_k^b(x) + \int m_{k|k-1}(x|\bar{x})p_{s,k}(\bar{x})\mu_{k-1}(\bar{x})d\bar{x}, \quad (2)$$

$$\mu_k(x) = \mu_k^\phi(x) + \sum_{z \in Z_k} \frac{\mu_k^z(x)}{\mu_k^{\text{fa}}(z) + \int \mu_k^z(x)dx}, \quad (3)$$

with

$$\begin{aligned} \mu_k^\phi(x) &= (1 - p_{d,k}(x))\mu_{k|k-1}(x), \\ \mu_k^z(x) &= p_{d,k}(x)g_k(z|x)\mu_{k|k-1}(x), \end{aligned}$$

where $\mu_{k|k-1}(\cdot)$ and $\mu_k(\cdot)$ are, respectively, the predicted and updated intensity functions;

$\mu_k^b(\cdot)$ and $\mu_k^{\text{fa}}(\cdot)$ are, respectively, the intensity functions of newborn objects and false alarms;

$Z_{1:k}$ is the sequence of multi-object observations collected by time k , where Z_k is a set of single-object measurements collected at time k ;

$g_k(\cdot|\cdot)$ is the single-object measurement likelihood;

$p_{s,k}(\cdot)$ and $p_{d,k}(\cdot)$ are, respectively, the probability of an object survival and its probability of detection;

$m_{k|k-1}(\cdot|\cdot)$ is the single-object Markov transition kernel, describing the time evolution of an object.

III. STATISTICS FOR THREAT ASSESSMENT

This section introduces the first- and second-order statistics of the aggregated threat level for the *updated* point process Φ_k

²In the literature originating from Mahler's Finite Set Statistics (FISST) framework [12], an alternative construction of simple point processes is a random finite set (RFS), a random object whose realisations are sets of points $\{x_1, \dots, x_n\}$, in which the elements are by construction *unordered*.

at some arbitrary time $k \geq 0$ using the information available from the PHD filter.

The combined threat of a population of objects is modelled through the *aggregated threat level* $\mathcal{T} : \mathcal{X} \rightarrow \mathbb{R}_0^+$, i.e. a population of targets with states $\varphi = (x_{1:n})$ has a threat level given by the scalar $\mathcal{T}(\varphi)$. As a consequence, the threat level of a population described by a point process Φ is described by the real-valued random variable

$$T_\Phi = \mathcal{T} \circ \Phi, \quad (4)$$

where \circ denotes the function composition operator.

As for usual real-valued random variables, we can describe T_Φ with its first moment or mean $\mathbb{E}[T_\Phi]$ and its second central moment or variance $\text{var}[T_\Phi]$, given by

$$\mathbb{E}[T_\Phi] \triangleq \int_{\mathcal{X}} \mathcal{T}(\varphi)P_\Phi(d\varphi) \text{ and} \quad (5)$$

$$\text{var}[T_\Phi] \triangleq \mathbb{E}[T_\Phi^2] - (\mathbb{E}[T_\Phi])^2 \quad (6)$$

$$= \int_{\mathcal{X}} \mathcal{T}^2(\varphi)P_\Phi(d\varphi) - \left(\int_{\mathcal{X}} \mathcal{T}(\varphi)P_\Phi(d\varphi) \right)^2. \quad (7)$$

The explicit expressions of these moments can be difficult to obtain in the general case, so in the scope of this paper we shall limit ourselves to the case of cumulative threat functions [14], [15], [16], i.e., at time k

$$\mathcal{T}_k(\varphi) = \sum_{x \in \varphi} \tau_k(x), \quad (8)$$

where τ_k is a function $\tau_k : \mathbf{X} \rightarrow [0, 1]$ evaluating the threat level of an individual object with state x [5], [17], [7].

Theorem III.1 (Mean cumulative threat level [9]).

Under the assumptions of the PHD filter and considering cumulative threat as in (8), the mean cumulative threat level of the updated point process Φ_k is given by

$$\mathbb{E}[T_{\Phi_k}] = \int \tau_k(x)\mu_k^\phi(x)dx + \sum_{z \in Z_k} \frac{\int \tau_k(x)\mu_k^z(x)dx}{\mu_k^{\text{fa}}(z) + \int \mu_k^z(x)dx}. \quad (9)$$

This result was first obtained by Mahler in [9, Eq. 35], and presented here for the sake of completeness.

Theorem III.2 (Variance in the cumulative threat level).

Under the assumptions of the PHD filter and considering cumulative threat as in (8), the variance in the cumulative threat level of the updated point process Φ_k is given by

$$\begin{aligned} \text{var}[T_{\Phi_k}] &= \int \tau_k^2(x)\mu_k^\phi(x)dx \\ &+ \sum_{z \in Z_k} \left[\frac{\int \tau_k^2(x)\mu_k^z(x)dx}{\mu_k^{\text{fa}}(z) + \int \mu_k^z(x)dx} - \left(\frac{\int \tau_k(x)\mu_k^z(x)dx}{\mu_k^{\text{fa}}(z) + \int \mu_k^z(x)dx} \right)^2 \right]. \end{aligned} \quad (10)$$

This theorem is the main result of this paper. Its proof is given in Appendix.

When interest lies in a specific region $B \subset \mathbf{X}$ the function τ_k can be selected to be the indicator function 1_B defined

such that $1_B(x) = 1$ if $x \in B$, $1_B(x) = 0$ otherwise. The cumulative threat level then reduces to the regional statistics describing the number of objects in B [10, Eq. 34 and 35].

IV. NUMERICAL EXAMPLES

The computation of the threat statistics impose no constraint on the implementation of the PHD filter. In this paper, an SMC-PHD filter [18] was used. The details of implementation are, however, omitted for the sake of brevity.

A. Simulation Setup

We consider a scenario where sensor is used to estimate a cumulative threat level generated by objects evolving in a specified surveillance area. In simulation we adopt the surveillance area to be a disk centred at the origin with radius 2000 m as depicted on Figure 1. The state of objects is described by $x = [x, y, \dot{x}, \dot{y}]^T$, where $[x, y]$ is a location component and $[\dot{x}, \dot{y}]$ is a velocity component, and T denotes the matrix transposition. The subset of \mathbb{R}^4 that falls in the surveillance area is the state space \mathbf{X} . The state transitions follow a nearly constant velocity motion model and (slight) additive zero mean process noise after getting initiated uniformly on the edge of the surveillance area, the initial velocities are chosen such that the targets are oriented towards the sensor with speeds uniformly distributed in $[10, 40] \text{ m s}^{-1}$. The birth model is Poisson with birth rate equal to 1. The probability of object survival between time steps is $p_s = 0.99$.

A radar-like sensor is static and located at the origin. The sensor's field of view covers the whole position subspace and the interval of range-rates $[-100, 100] \text{ m s}^{-1}$. The standard deviations in range, bearing and range-rate are selected as 5 m, 3° , and 4 m s^{-1} respectively. The false alarms are generated from a Poisson process with rate equal to 20 and uniform distribution over the field of view. The probability of detection is uniform across the field of view $p_d = 0.98$.

Figure 1 illustrates the particle representation of the intensity μ_k in the running SMC-PHD filter.

B. Threat Assessment Details

The threat level of x is evaluated w.r.t. to a point of interest $x_o \in \mathbf{X}$ and a region of interest $B \subset \mathbf{X}$ by

$$\tau(x) = 1_B(x) \exp\left(-\frac{d(x, x_o)}{\alpha} - \frac{b^2(x, x_o)}{2\beta^2}\right), \quad (11)$$

a time-invariant function (hence the index k in τ_k is dropped), where $1_B(x)$ evaluates whether x belongs to the region B ; $d(x, x_o) = \sqrt{(x - x_o)^2 + (y - y_o)^2}$ is the distance between the object and the point which is related to the object's capability to inflict negative effect; the object's direction $b(x, x_o) = |\text{atan2}(\dot{y}, \dot{x}) - \text{atan2}(x_o - x, y_o - y)|$ w.r.t. the point is related to object's intention to act hostile, where $\text{atan2}(y, x)$ is the four-quadrant inverse tangent function; α and β are positive-valued scaling parameters.

In preparation to a sensor management scenario [19], [2], we wish to estimate the threat level in various regions in order to be able to focus sensing resources in the region that needs

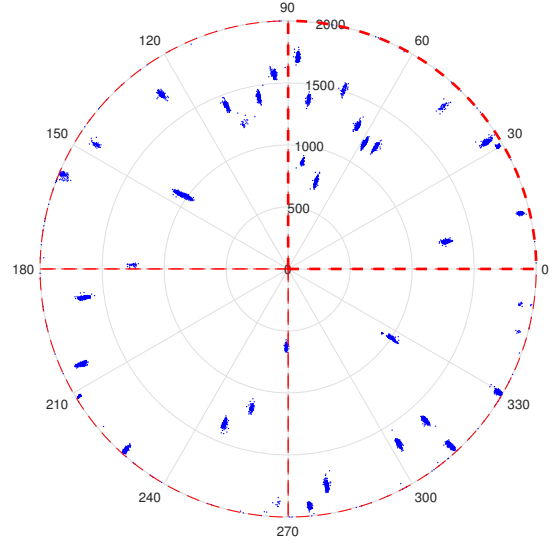


Fig. 1. An example of the updated intensity μ_k in the running PHD filter in the simulated scenario. The particles (blue dots) are projected on the subspace of \mathbf{X} consisting of position variables only. The regions of interest (quadrants) are depicted with red dashed lines and numbered counter-clockwise with the first sector plotted with a thicker line. The sensor is located at the centre of the surveillance area.

it the most. The four considered regions are the four quadrants illustrated in Figure 1. The point of interest is selected to coincide with the sensor location.

C. Simulation Results

We consider statistics of cumulative threat level in the surveillance area divided into four regions as depicted on Figure 1 for the duration of 45 s. The threat level of individual objects is calculated using (11) with sensitivity parameters $\alpha = 2000 \text{ m}$ and $\beta = 0.5$.

In Figure 2, we demonstrate the mean threat level for each of the sectors (black plain line), together with the ground truth (red plain line). The variance in threat level is used to quantify the uncertainty in the estimated threat level. Specifically, we demonstrate confidence intervals (black dashed lines) as ± 1 square root of the threat level variance which is a standard deviation. We note that the ground truth falls within the confidence interval during the course of scenario, this demonstrates that results of threat assessment in this case are reliable.

V. CONCLUSION

This paper explores the estimation of the cumulative threat level of a population of objects through its first- and second-order statistics, in order to assess threat level uncertainty and provide a measure of confidence in the estimated threat. It provides a principled construction of the second-order central moment or variance of the cumulative threat level, and an explicit expression from the output of the data update step of the PHD filter. The behaviour of the developed statistic is illustrated on a simulated scenario, where the statistics of the cumulative threat are computed in four quadrants (regions) of the surveillance area.

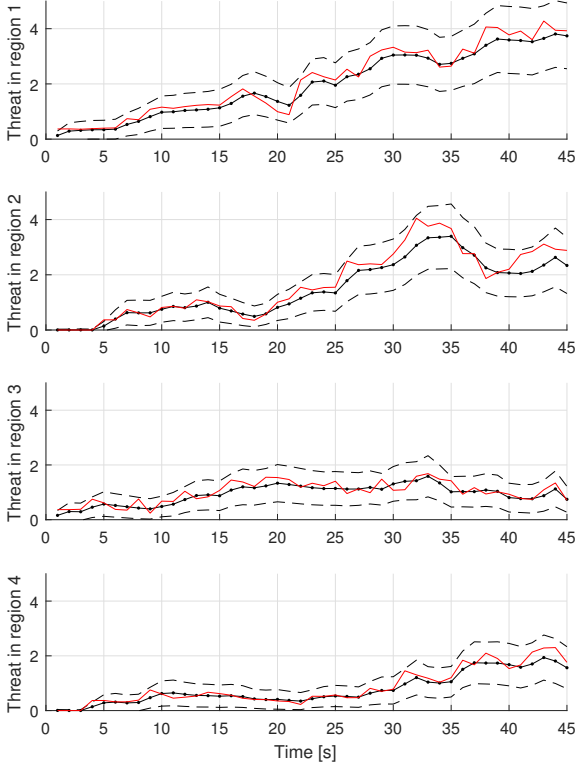


Fig. 2. Mean cumulative threat level and ± 1 standard deviation (square root of the variance) in regions from 1 to 4. The ground truth value of the threat level is plotted with plain red line. The results are averages over 60 Monte Carlo runs.

APPENDIX: PROOF OF THEOREM III.2

Proof. The variance in the estimated threat level T_k is defined by

$$\text{var}[T_k] \triangleq \mathbb{E}[T_k^2] - (\mathbb{E}[T_k])^2. \quad (12)$$

Let us first focus on the expected value $\mathbb{E}[T_k]$ of the threat level T_k . From (5) and (8) we can write

$$\mathbb{E}[T_k] = \int_{\mathcal{X}} \left(\sum_{x \in \varphi} \tau_k(x) \right) P_{\Phi_k}(\mathrm{d}\varphi), \quad (13a)$$

and then using Campbell's theorem [11, p. 103] yields

$$\mathbb{E}[T_k] = \int \tau_k(x) \mu_k(x) \mathrm{d}x, \quad (13b)$$

where $\mu_k(x)$ is the updated intensity of the process (3), so

$$\mathbb{E}[T_k] = \int \tau_k(x) \mu_k^\phi(x) \mathrm{d}x + \sum_{z \in Z} \frac{\int \tau_k(x) \mu_k^z(x) \mathrm{d}x}{\mu_k^{\text{fa}}(z) + \int \mu_k^z(x) \mathrm{d}x}. \quad (13c)$$

This is the result in (9) that was obtained in [9].

Next we focus on the expected value $\mathbb{E}[T_k^2]$ of the squared threat level T_k^2 . Once again, from (5) and (8) we have

$$\mathbb{E}[T_k^2] = \int_{\mathcal{X}} \left(\sum_{x \in \varphi} \tau_k(x) \right)^2 P_{\Phi_k}(\mathrm{d}\varphi) \quad (14a)$$

$$= \int_{\mathcal{X}} \left(\sum_{x_i, x_j \in \varphi} \tau_k(x_i) \tau_k(x_j) \right) P_{\Phi_k}(\mathrm{d}\varphi) \quad (14b)$$

$$= \int_{\mathcal{X}} \left(\sum_{x \in \varphi} \tau_k^2(x) \right) P_{\Phi_k}(\mathrm{d}\varphi) + \int_{\mathcal{X}} \left(\sum_{x_i, x_j \in \varphi}^{\neq} \tau_k(x_i) \tau_k(x_j) \right) P_{\Phi_k}(\mathrm{d}\varphi), \quad (14c)$$

where \sum^{\neq} stands for the summation over all pairs of *distinct* points x in a sequence φ . Using Campbell's theorem yields

$$\mathbb{E}[T_k^2] = \int \tau_k^2(x) \mu_k(x) \mathrm{d}x + \iint \tau_k(x) \tau_k(\bar{x}) \nu_k^{(2)}(x, \bar{x}) \mathrm{d}x \mathrm{d}\bar{x}, \quad (14d)$$

where $\nu_k^{(2)}(x, \bar{x})$ is the second-order *factorial* moment density of the point process Φ_k [11, p. 37]. The density $\nu_k^{(2)}(x, \bar{x})$ can be computed from the second-order *non-factorial* moment density, available for the updated PHD from [10, Eq. 31], using the expression [11, Eq. 4.3.4]. It yields

$$\begin{aligned} \nu_k^{(2)}(x, \bar{x}) &= \mu_k^\phi(x) \mu_k^\phi(\bar{x}) + \mu_k^\phi(x) \sum_{z \in Z} \frac{\mu_k^z(\bar{x})}{\mu_k^{\text{fa}}(z) + \int \mu_k^z(x) \mathrm{d}x} \\ &+ \mu_k^\phi(\bar{x}) \sum_{z \in Z} \frac{\mu_k^z(x)}{\mu_k^{\text{fa}}(z) + \int \mu_k^z(x) \mathrm{d}x} \\ &+ \sum_{z, \bar{z} \in Z}^{\neq} \left(\frac{\mu_k^z(x)}{\mu_k^{\text{fa}}(z) + \int \mu_k^z(x) \mathrm{d}x} \right) \left(\frac{\mu_k^{\bar{z}}(\bar{x})}{\mu_k^{\text{fa}}(\bar{z}) + \int \mu_k^{\bar{z}}(x) \mathrm{d}x} \right). \end{aligned} \quad (15)$$

Substituting the expressions for $\nu_k^{(2)}(x, \bar{x})$ from (15) and for $\mu_k(x)$ from (3) into (14d), we can write

$$\begin{aligned} \mathbb{E}[T_k^2] &= \int \tau_k^2(x) \mu_k^\phi(x) \mathrm{d}x + \sum_{z \in Z} \frac{\int \tau_k^2(x) \mu_k^z(x) \mathrm{d}x}{\mu_k^{\text{fa}}(z) + \int \mu_k^z(x) \mathrm{d}x} \\ &+ \left(\int \tau_k(x) \mu_k^\phi(x) \mathrm{d}x \right)^2 \\ &+ 2 \int \tau_k(x) \mu_k^\phi(x) \mathrm{d}x \sum_{z \in Z} \frac{\int \tau_k(\bar{x}) \mu_k^z(\bar{x}) \mathrm{d}\bar{x}}{\mu_k^{\text{fa}}(z) + \int \mu_k^z(x) \mathrm{d}x} \\ &+ \sum_{z, \bar{z} \in Z}^{\neq} \frac{\left(\int \tau_k(x) \mu_k^z(x) \mathrm{d}x \right) \left(\int \tau_k(\bar{x}) \mu_k^{\bar{z}}(\bar{x}) \mathrm{d}\bar{x} \right)}{\left(\mu_k^{\text{fa}}(z) + \int \mu_k^z(x) \mathrm{d}x \right) \left(\mu_k^{\text{fa}}(\bar{z}) + \int \mu_k^{\bar{z}}(x) \mathrm{d}x \right)}. \end{aligned} \quad (16)$$

Finally, substituting (17) and (13c) into (12) yields the result. \square

REFERENCES

- [1] A. N. Steinberg and C. L. Bowman, "Revisions to the JDL data fusion model," in *Handbook of Multisensor Data Fusion: Theory and Practice, Second Edition*. CRC Press, 2008, pp. 45–67.
- [2] S. F. Page, J. P. Oldfield, and P. Thomas, "Towards integrated threat assessment and sensor management: Bayesian multi-target search," in *IEEE International Conference on Multisensor Fusion and Integration for Intelligent Systems (MFI)*. IEEE, 2016, pp. 44–51.
- [3] J. J. Salerno, S. J. Yang, I. Kadar, M. Sudit, G. P. Tadda, and J. Holsopple, "Issues and challenges in higher level fusion: Threat/impact assessment and intent modeling (a panel summary)," in *Information Fusion (FUSION), 2010 13th Conference on*. IEEE, 2010, pp. 1–17.
- [4] A. H. Jazwinski, *Stochastic processes and filtering theory*. Dover Publications Inc., 2007.
- [5] N. Okello and G. Thorns, "Threat assessment using Bayesian networks," in *Sixth International Conference of Information Fusion, 2003. Proceedings of the*, vol. 2, July 2003, pp. 1102–1109.
- [6] R. F. Riggs, "The effects of sensor errors in certain marine collision avoidance and threat assessment systems," *Navigation*, vol. 21, no. 1, pp. 16–34, 1974.
- [7] F. Katsilieris, H. Driessen, and A. Yarovoy, "Threat-based sensor management for target tracking," *IEEE Transactions on Aerospace and Electronic Systems*, vol. 51, no. 4, pp. 2772–2785, 2015.
- [8] E. G. Little and G. L. Rogova, "An ontological analysis of threat and vulnerability," in *Information Fusion, 2006 9th International Conference on*. IEEE, 2006, pp. 1–8.
- [9] R. P. Mahler, "Target preference in multitarget sensor management: A unified approach," in *Defense and Security*. International Society for Optics and Photonics, 2004, pp. 210–221.
- [10] E. Delande, M. Uney, J. Houssineau, and D. E. Clark, "Regional variance for multi-object filtering," *IEEE Transactions on Signal Processing*, vol. 62, no. 13-16, pp. 3415–3428, 2014.
- [11] D. Stoyan, W. S. Kendall, and J. Mecke, *Stochastic geometry and its applications*. John Wiley & Sons, 1995.
- [12] R. P. Mahler, "Multitarget bayes filtering via first-order multitarget moments," *IEEE Transactions on Aerospace and Electronic systems*, vol. 39, no. 4, pp. 1152–1178, 2003.
- [13] R. P. Mahler, *Statistical multisource-multitarget information fusion*. Artech House, Inc., 2007.
- [14] W. J. Horrey, C. D. Wickens, R. Strauss, A. Kirlik, and T. R. Stewart, "Supporting situation assessment through attention guidance and diagnostic aiding: The benefits and costs of display enhancement on judgment skill," *Adaptive perspectives on human technology interaction: Methods and models for cognitive engineering and human-computer interaction*, pp. 55–70, 2006.
- [15] M. Witkowski, G. White, P. Louvieris, G. Gorbil, E. Gelenbe, and L. Dodd, "High-level information fusion and mission planning in highly anisotropic threat spaces," in *11th International Conference on Information Fusion, 2008*. IEEE, 2008, pp. 1–8.
- [16] F. Johansson and G. Falkman, "Real-time allocation of firing units to hostile targets," *Journal of Advances in Information Fusion*, vol. 6, no. 2, pp. 187–199, 2011.
- [17] F. Johansson and G. Falkman, "A Bayesian network approach to threat evaluation with application to an air defense scenario," in *Information Fusion, 2008 11th International Conference on*. IEEE, 2008, pp. 1–7.
- [18] B.-N. Vo, S. Singh, and A. Doucet, "Sequential Monte Carlo methods for multitarget filtering with random finite sets," *IEEE Transactions on Aerospace and electronic systems*, vol. 41, no. 4, pp. 1224–1245, 2005.
- [19] M. Andrecki, E. D. Delande, J. Houssineau, and D. E. Clark, "Sensor management with regional statistics for the PHD filter," in *Sensor Signal Processing for Defence (SSPD), 2015*. IEEE, 2015, pp. 1–5.